4th MASHCON, Hamburg - Uliczka et al. (eds) - © 2016 Bundesanstalt für Wasserbau ISBN 978-3-939230-38-0 (Online)
DOI: 10.18451/978-3-939230-38-0_33

SHALLOW WATER EFFECTS ON LONGITUDINAL COMPONENTS OF HYDRODYNAMIC DERIVATIVES

Y Furukawa, H Ibaragi, Y Nakiri and **K Kijima,** Kyushu University, Fukuoka, Japan

SUMMARY

In order to evaluate ship manoeuvrability in shallow water condition by numerical simulation based on MMG mathematical model, it is important to use hydrodynamic coefficients on which shallow water effects are considered properly. The authors have carried out captive model tests to measure hydrodynamic forces acting on the bare hulls of eighteen model ships of tankers, bulk carriers and so on both in deep and shallow water conditions and accumulated the measured forces as a database. In this paper, the authors present shallow water effects on the longitudinal components of hydrodynamic derivatives based on the analysis of the measured forces in the database. The variation of the longitudinal components of hydrodynamic derivatives by principal particulars of ships or water depth is investigated.

NOMENCLATURE

B	Breadth of ship (m)
C_b	Block coefficient of ship (-)
H	Depth of water (m)
L	Length of ship (m)
m	Mass of ship (kg)
m_y	Lateral component of added mass of ship (kg)
R_0	Resistance of ship in forward straight motion measured at midship (N)
r	Yaw rate (rad/s)
T	Draught of ship (m)
U	Ship speed at midship (m/s)
v	Lateral component of ship speed at midship (m/s)
X_H	Longitudinal component of hydrodynamic force acting on ship hull measured at midship (N)
$X'_{\beta r}$, X'_{uu}, X'_{vv}, X'_{vvvv}, X'_{vr}, X'_{rr}, X'_{vvr}	Hydrodynamic derivatives (-)
x_G	Longitudinal coordinate of centre of gravity of ship (m)
β	Drift angle (rad)
ρ	Density of water (kg/m^3)
$'$	Non-dimensional quantity (-)

1 INTRODUCTION

In order to evaluate ship manoeuvrability in shallow water condition by numerical simulation based on MMG (Manoeuvring Mathematical Modelling Group in Japan Towing Tank Committee) mathematical model, it is important to use hydrodynamic coefficients on which shallow water effects are considered properly. Performing captive model tests is a steady way to get the hydrodynamic coefficients but the number of facilities which have capability to conduct captive model tests in shallow water condition is few. There are several published papers [1-6] reporting the results of captive model tests both in deep and shallow water conditions. In these papers, the influence of water depth on lateral force and yawing moment is mainly paid attention and the discussion of water depth effect on longitudinal force is often omitted.

CFD calculations [7-10] are promising methods to evaluate the shallow water effect on hydrodynamic forces, but it will still take a while before captive model tests are replaced with CFD and it is also a time consuming method. Therefore an empirical prediction method based on the database of measured hydrodynamic forces by captive model tests would be still useful at a design stage.

The authors have carried out captive model tests to measure longitudinal and lateral forces and yawing moment acting on the bare hulls of ten model ships both in deep and shallow water conditions and accumulated the measured forces as a database. The basic settings of the ratio of water depth (H) for draught (T) in the shallow water conditions are $H/T = 2.0$, 1.5 and 1.3 or 1.2. Based on the database, some empirical formulae for estimating linear hydrodynamic derivatives for lateral force and yawing moment in deep and shallow water conditions had been proposed by the authors [11].

As for the longitudinal components of hydrodynamic derivatives, there are few empirical methods to estimate them even in deep water condition. An estimation chart for X'_{vr} was presented by Hasegawa [12] and Yoshimura et al. [13] proposed regression formulae for the hydrodynamic derivatives of longitudinal force based on their hydrodynamic force database.

In this paper, the authors present shallow water effects on the longitudinal components of hydrodynamic derivatives based on the analysis of the measured forces in the database. The variation of the longitudinal components of hydrodynamic derivatives by principal particulars of ships or water depth is investigated.

Table 1. Principal dimensions of model ships and conditions of water depth / draught ratio.

Ship	Ship type	L (m)	L/B	B/T	C_b	H/T 6.0	2.0	1.5	1.3	1.2
Ship A	Tanker	2.5	5.5175	2.7885	0.8099	✓	✓	✓		✓
Ship B	Tanker	2.5	5.5175	2.7885	0.8101	✓				
Ship C	Tanker	2.5	6.1320	2.4039	0.8310	✓		✓		✓
Ship D	Tanker	2.5	5.7405	2.7686	0.8023	✓	✓	✓	✓	
Ship E	Bulk carrier	2.5	5.0000	4.7619	0.8232	✓	✓	✓		✓
Ship F	Bulk carrier	2.5	5.5556	2.6627	over 0.8	✓		✓		✓
Ship G	Bulk carrier	2.5	5.3487	3.3079	over 0.8	✓	✓	✓		✓
Ship H	Bulk carrier	2.5	5.2521	3.9016	over 0.8	✓	✓			
Ship I	Bulk carrier	2.5	5.6433	2.8397	over 0.8	✓				
Ship J	Bulk carrier	2.5	5.3763	3.3696	over 0.8	✓				
Ship K	Bulk carrier	2.5	6.7150	3.3723	over 0.8	✓				
Ship L	Bulk carrier	2.5	5.3717	3.3725	over 0.8	✓				
Ship M	Coal carrier	2.5	5.5816	3.9463	0.8123	✓		✓		✓
Ship N	Cargo carrier	2.5	5.8221	2.6905	0.8271	✓				
Ship O	Cargo carrier	2.5	6.1244	2.3816	0.7727	✓	✓	✓	✓	
Ship P	Chemical tanker	2.5	5.9552	2.7384	0.7513	✓	✓	✓		
Ship Q	Cable layer	2.5	6.4817	2.8935	0.6326	✓				
Ship R	Container carrier	3.0	6.8966	2.6703	0.5717	✓				

2 MEASURED HYDRODYNAMIC FORCES ACCUMULATED IN A DATABASE

2.1 MODEL SHIPS AND TEST CONDITIONS

The authors have carried out captive model tests to measure longitudinal and lateral forces and yawing moment acting on the bare hulls of ten model ships shown in Table 1 both in deep and shallow water conditions. Most of them are full ships of which C_b is over 0.8. Captive model tests in deep water condition have been also conducted for eight model ships in Table 1. These tests were performed at either old or new Seakeeping and Manoeuvring Basin of Kyushu University. A rotating arm and a towing carriage were used at the old basin (1959-2007) and a CPMC (computerized planar mechanism carriage) was used at the new basin (2008-) to execute oblique towing test and circular motion test. Measured longitudinal forces were nondimensionalized by using the following equation and accumulated in a database.

$$X'_H = \frac{X_H}{(1/2)\rho LTU^2} \tag{1}$$

The basic settings of the conditions of drift angle β, non-dimensional yaw rate r' and water depth / draught ratio H/T are as the following. The range of drift angle is $-10^\circ \le \beta \le 20^\circ$ and non-dimensional yaw rate are varied from 0.0 to 1.0. The step sizes of β and r' are various for each model ship. The value of H/T for deep water condition is normally set greater than 6.0 and those in shallow water conditions are 2.0, 1.5 and 1.3 or 1.2.

2.2 EXAMPLES OF MEASURED FORCES

Symbols in Figure 1 show non-dimensional longitudinal forces $X'_H(\beta, r')$ of the ships A, C and M in deep water condition. The measured forces include inertia force components. It is observed that non-dimensional longitudinal force $X'_H(\beta, 0.0)$ in pure drift motion with small drift angle is almost constant for all ships. As the value of drift angle becomes larger than 10º, the absolute value of X'_H becomes slightly smaller. By paying attention to the value of $X'_H(0^\circ, r')$ on a vertical axis, it is found that its variation for non-dimensional yaw rate is quite different among the ships A, C and M. The value of $X'_H(0^\circ, r')$ for the ship C is almost constant regardless of the value of non-dimensional yaw rate. The absolute value of $X'_H(0^\circ, r')$ for the ship A decreases as non-dimensional yaw rate becomes large. In contrast, that of the ship M increases for the growth of non-dimensional yaw rate.

Longitudinal forces of the ship A in shallow water conditions are shown by symbols in Figure 2. As the depth of water becomes shallow, the nonlinearity of X'_H for drift angle appears remarkably. The value of $X'_H(\beta, 0.0)$ tends to change into the positive direction with the increase of drift angle. This phenomenon was also presented in the references [14-16]. In the condition of $H/T = 1.2$, $X'_H(\beta, 0.0)$ with large drift angle takes a positive value. It means the direction of longitudinal force turns in thrust direction. Although there is the difference in degree, the nonlinearity of X'_H for drift angle is observed for all model ships in shallow water condition.

3 MATHEMATICAL MODELS AND HYDRODYNAMIC DERIVATIVES

3.1 MATHEMATICAL MODELS FOR LONGITUDINAL FORCE ACTING ON SHIP HULL

There are several kinds of mathematical model used for the analysis of longitudinal force acting on a ship hull.

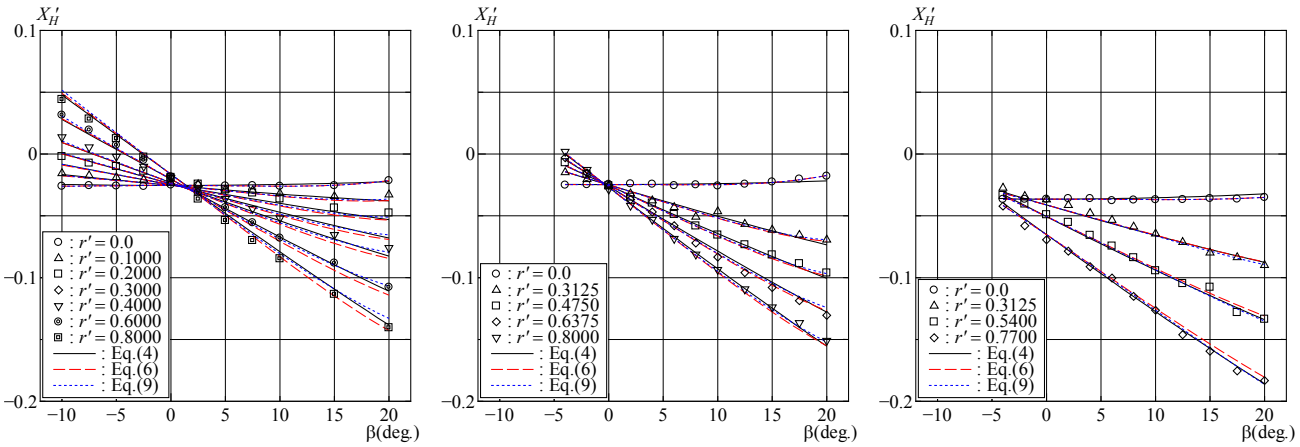

(a) Ship A (b) Ship C (c) Ship M

Figure 1. Measured hydrodynamic forces and fitting curves with mathematical models shown by Eqs. (4), (6) and (9) in deep water condition (Ships A, C and M).

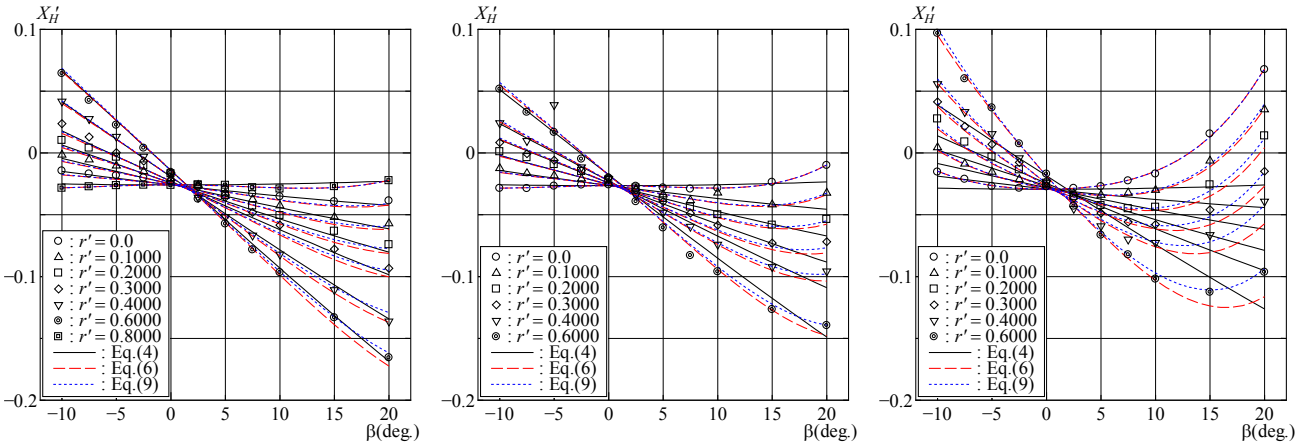

(a) $H/T = 2.0$ (b) $H/T = 1.5$ (c) $H/T = 1.2$

Figure 2. Measured hydrodynamic forces and fitting curves with mathematical models shown by Eqs. (4), (6) and (9) in shallow water conditions (Ship A).

The authors have been using the following expression [17],

$$X'_H = X'_{uu}\cos^2\beta + \{X'_{\beta r} - (m' + m'_y)\}r'\sin\beta + (X'_{rr} + x'_G m')r'^2, \tag{2}$$

where,

$$m', m'_y = \frac{m, m_y}{(1/2)\rho L^2 T}, \quad r' = \frac{rL}{U}, \quad x'_G = \frac{x_G}{L}. \tag{3}$$

The mathematical model shown by Eq.(2) is formulated using drift angle β and non-dimensional yaw rate r'. Ship mass and added mass components are included in the second term of the right side. X'_{uu} is a hydrodynamic derivative which indicates non-dimensional resistance of ship in forward straight motion. A hydrodynamic derivative $X'_{\beta r}$ is a coupling term of β and r' which represents the variation of the slope of longitudinal force for drift angle β due to yaw motion. X'_{rr} is a derivative which shows the change of resistance due to yaw motion. Eq.(2) can be transformed to the following form.

$$\begin{aligned} X'_H &= X'_{uu} - X'_{uu}\sin^2\beta + \{X'_{\beta r} - (m' + m'_y)\}r'\sin\beta \\ &\quad + (X'_{rr} + x'_G m')r'^2 \\ &= X'_{uu} - X'_{uu}v'^2 - \{X'_{\beta r} - (m' + m'_y)\}v'r' \\ &\quad + (X'_{rr} + x'_G m')r'^2, \end{aligned} \tag{4}$$

where,

$$v' = \frac{v}{U} = \frac{-U\sin\beta}{U} = -\sin\beta. \tag{5}$$

It is understood from Eq.(4) that the mathematical model contains the term of v'^2 which is the quadratic component of drift motion and non-dimensional hull resistance X'_{uu} is used in substitution for a derivative for the term. X'_{uu} is often measured in resistance test, then the estimates of the value of $X'_{\beta r}$ and X'_{rr} are required to simulate ship's manoeuvring motion using the mathematical model shown by Eq.(4).

On the other hand, the following expression is proposed in the reference [18] as the standard of mathematical

model for longitudinal force acting on a ship hull in manoeuvring motion,

$$X'_H = -R'_0 + X'_{vv}v'^2 + (X'_{vr} + m' + m'_y)v'r' + (X'_{rr} + x'_G m')r'^2 + X'_{vvvv}v'^4, \quad (6)$$

where,

$$R'_0 = \frac{R_0}{(1/2)\rho LTU^2}. \quad (7)$$

Drift motion is represented by non-dimensional sway velocity v' instead of drift angle β in Eq.(6). Comparing the mathematical models shown by Eq.(6) with the first model shown by Eq.(4), it is understood that an independent derivative X'_{vv} has been adopted for v'^2 and an additional derivative X'_{vvvv} for v'^4 has been introduced. Thus, the estimates of the value of four derivatives X'_{vv}, X'_{vr}, X'_{rr} and X'_{vvvv} are necessary to carry out numerical simulation.

Furthermore the following relations exist between the hydrodynamic derivatives used in the first model shown by Eq.(4) and the second model shown by Eq.(6),

$$X'_{uu} = -R'_0, \quad X'_{\beta r} = -X'_{vr}. \quad (8)$$

In this paper, the measured forces are analyzed by using both mathematical models shown by Eqs.(4) and (6).

3.2 FITTED RESULTS BY THE MATHEMATICAL MODELS

Fitting curves with hydrodynamic derivatives obtained by analyses using the mathematical models shown by Eqs.(4) and (6) for deep water condition are shown by black solid lines and red broken lines respectively in Figure 1 for the ships A, C and M. Both mathematical models can reproduce the measured force well for the three ships in deep water condition.

Fitting curves for the ship A in shallow water conditions are also shown in Figure 2. There exists clear difference between black solid lines and red broken lines representing the two mathematical models. Agreement of measured forces and the fitted results of the first model is not good especially for the conditions of $H/T = 1.5$ and 1.2. As stated in the previous section, the nonlinearity of X'_H for drift angle appears remarkably in shallow water conditions. On the other hand, a derivative for v'^2 in the first model shown by Eq.(4) is substituted by X'_{uu}. For this reason, the nonlinearity of X'_H for drift angle could not be expressed well in shallow water conditions by the first model.

In contrast, the second model shown by Eq.(6) having terms of v'^2 and v'^4 can reproduce the measured forces in shallow water conditions better than the first model. However, it is observed that agreement between measured and fitted results become worse as the value of non-dimensional yaw rate increase. This arises from strengthened nonlinearity for drift angle at large yaw motion, thus the discrepancy can be made small by adding a term of X'_{vvr} which represents the variation of X'_{vv} for r' as the following,

$$X'_H = -R'_0 + X'_{vv}v'^2 + (X'_{vr} + m' + m'_y)v'r' + (X'_{rr} + x'_G m')r'^2 + X'_{vvvv}v'^4 + X'_{vvr}v'^2 r'. \quad (9)$$

Fitting curves with a mathematical model shown by Eq.(9) are shown in blue dotted lines in Figures 1 and 2. Obviously difference between measured and fitted results becomes smaller in shallow water conditions, though extra effort to define the value of X'_{vvr} is required. It is up to required precision of X'_H whether X'_{vvr} is adopted.

In order to get better agreement between measured forces and fitted results by the first mathematical model, the terms of X'_{vv}, X'_{vvvv} and X'_{vvr} should be introduced in Eq.(4). It means that the first mathematical model will have the same form of the third model shown by Eq.(9). Consequently, hydrodynamic derivatives for the third mathematical model shown by Eq.(9) will be presented hereafter.

4 HYDORDYNAMIC DERIVATIVES IN DEEP AND SHALLOW WATER CONDITIONS

4.1 DERIVED HYDRODYNAMIC DERIVATIVES

The hydrodynamic derivatives were derived based on the mathematical model shown by Eq.(9) for the model ships presented in Table 1 using the database of hydrodynamic forces. After having derived the term of $X'_{vr} + m' + m'_y$, non-dimensional mass m' ($= 2C_bB/L$) was excluded from the value of the term. The values of the hydrodynamic derivatives are listed in Table 2 for deep and shallow water conditions.

4.2 HYDRODYNAMIC DERIVATIVES IN DEEP WATER CONDITION

It is ideal to evaluate the relation between the hydrodynamic derivatives and ship type while focusing on a physical phenomenon such as the change of flow field around hull. However, available information from the database is only measured forces and the principal particulars of model ships. Hence correlation coefficients between the hydrodynamic derivatives and non-dimensional parameters comprised of principal particulars were investigated. The non-dimensional parameters used in the calculation of correlation coefficients are C_b, T/L, T/B, B/L and their combinations.

Figure 3 shows each derivative as the function of a parameter indicating the highest correlation and the values of correlation coefficients are shown in Table 3. The ships are classified in two groups of $C_b \geq 0.8$ and $C_b < 0.8$ in Figure 3. It is understood that there is low correlation between each derivative and corresponding non-dimensional parameter. Even $X'_{vr} + m'_y$ which

Table 2. Hydrodynamic derivatives in deep and shallow water conditions.

Ship	H/T	R'_0	$X'_{rr}+x'_G m'$	X'_{vv}	$X'_{vr}+m'_y$	X'_{vvvv}	X'_{vvr}
Ship A	6.0	0.0253	0.0140	-0.0397	0.1827	0.6223	0.1051
	2.0	0.0258	0.0183	-0.1179	0.2986	1.2758	0.1135
	1.5	0.0265	0.0242	-0.1349	0.4215	2.3799	0.1191
	1.2	0.0293	0.0300	0.3651	0.6572	3.9971	0.3213
Ship B	6.0	0.0265	0.0253	-0.0502	0.1727	0.6027	0.1270
Ship C	6.0	0.0246	-0.0035	-0.0265	0.2243	0.7598	0.0323
	1.5	0.0280	-0.0187	0.0674	0.5071	1.9752	0.0154
	1.2	0.0336	-0.0105	0.8000	0.7266	1.9941	0.4875
Ship D	6.0	0.0271	0.0009	-0.0937	0.1738	1.0924	-0.0376
	2.0	0.0307	-0.0216	0.1171	0.0830	-0.2930	-0.2408
	1.5	0.0309	-0.0177	0.1056	0.1817	1.2542	-0.3752
	1.3	0.0355	-0.0534	0.9500	0.4976	-0.2871	0.6037
Ship E	6.0	0.0350	-0.0150	-0.0725	0.1888	0.4541	0.1775
	2.0	0.0386	-0.0198	-0.1393	0.3277	1.1213	0.0765
	1.5	0.0436	-0.0173	-0.0772	0.4997	2.0665	0.3226
	1.2	0.0508	-0.0017	0.7917	0.7184	-0.3953	0.6163
Ship F	6.0	0.0246	0.0016	-0.0658	0.1862	0.9222	0.0795
	1.5	0.0306	-0.0019	-0.0107	0.4908	1.8417	0.3815
	1.2	0.0329	0.0075	0.4986	0.5862	3.4906	0.4833
Ship G	6.0	0.0279	0.0098	-0.0638	0.1475	0.5618	0.0559
	2.0	0.0285	-0.0154	-0.1149	0.2889	1.0689	0.1698
	1.5	0.0318	0.0012	-0.1323	0.4233	2.4418	0.3373
	1.2	0.0366	0.0283	0.6966	0.4962	1.5294	0.3436
Ship H	6.0	0.0327	-0.0045	-0.0149	0.1748	0.1539	0.1107
	2.0	0.0366	-0.0187	-0.1109	0.2923	0.6408	0.1691
Ship I	6.0	0.0253	-0.0206	-0.0680	0.1374	0.5743	0.1256
Ship J	6.0	0.0284	0.0211	-0.0567	0.1732	0.2650	0.0763
Ship K	6.0	0.0384	0.0017	-0.0941	0.2329	0.6866	0.3158
Ship L	6.0	0.0288	0.0044	-0.0008	0.2243	0.1031	0.1057
Ship M	6.0	0.0364	-0.0484	-0.0191	0.1524	0.2667	-0.0644
	1.5	0.0411	-0.0360	-0.0643	0.4000	1.6335	0.2078
	1.2	0.0510	0.0134	0.4233	0.6734	3.2333	-0.0570
Ship N	6.0	0.0255	-0.0034	-0.0909	0.2209	0.8040	-0.0117
Ship O	6.0	0.0202	-0.0377	0.0659	0.1085	-0.4098	0.0134
	2.0	0.0184	-0.0479	-0.1607	0.1771	0.9899	0.0763
	1.5	0.0172	-0.0453	-0.4233	0.3521	3.6515	0.3592
	1.3	0.0218	-0.0457	0.1134	0.4541	3.2435	0.6028
Ship P	6.0	0.0247	-0.0304	-0.0514	0.1724	0.4199	0.1472
	1.5	0.0288	-0.0233	-0.1280	0.4662	2.1014	0.4523
	1.2	0.0327	-0.0055	0.6756	0.5405	0.6160	0.4897
Ship Q	6.0	0.0201	-0.0272	-0.0500	0.0841	0.5013	-0.0041
Ship R	6.0	0.0161	-0.0379	-0.1590	0.1422	1.1370	0.1961

indicates the highest correlation among the derivatives, the value of its correlation coefficient is less than 0.7. However, it can be said that ships of which C_b is less than 0.8 might have negative $X'_{rr}+x'_G m'$.

Yoshimura et al. [13] proposed approximate formulae for the hydrodynamic derivatives of longitudinal force as function of C_bB/L based on their hydrodynamic force database which contains the measured data of medium high speed merchant ships and fishing vessels. The authors also calculated correlation coefficients of the derivatives and C_bB/L and they are presented in Table 4. The values of the correlation coefficients are less than the values shown in Table 3.

According to the results presented in Tables 3 and 4, it seems to be difficult to evaluate each hydrodynamic derivative based on an explanatory variable, therefore multiple regression analysis [19] were carried out using the non-dimensional parameters such as C_b, T/L, T/B, B/L and their combinations. For the purpose of practical use, the number of explanatory variables is limited in 3 or less

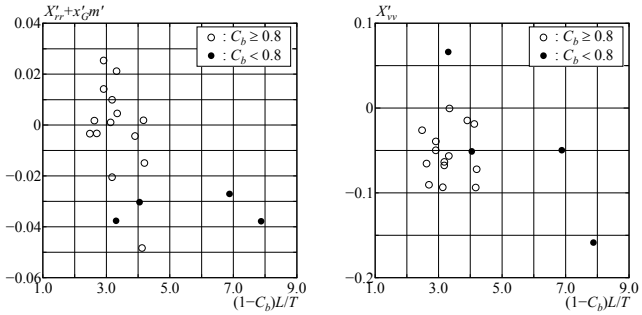

(a) $X'_{rr}+x'_Gm'$ (b) X'_{vv}

(c) $X'_{vr}+m'_y$ (d) X'_{vvvv}

(e) X'_{vvr}

Figure 3. Scattering diagrams of each hydrodynamic derivative for corresponding non-dimensional parameter.

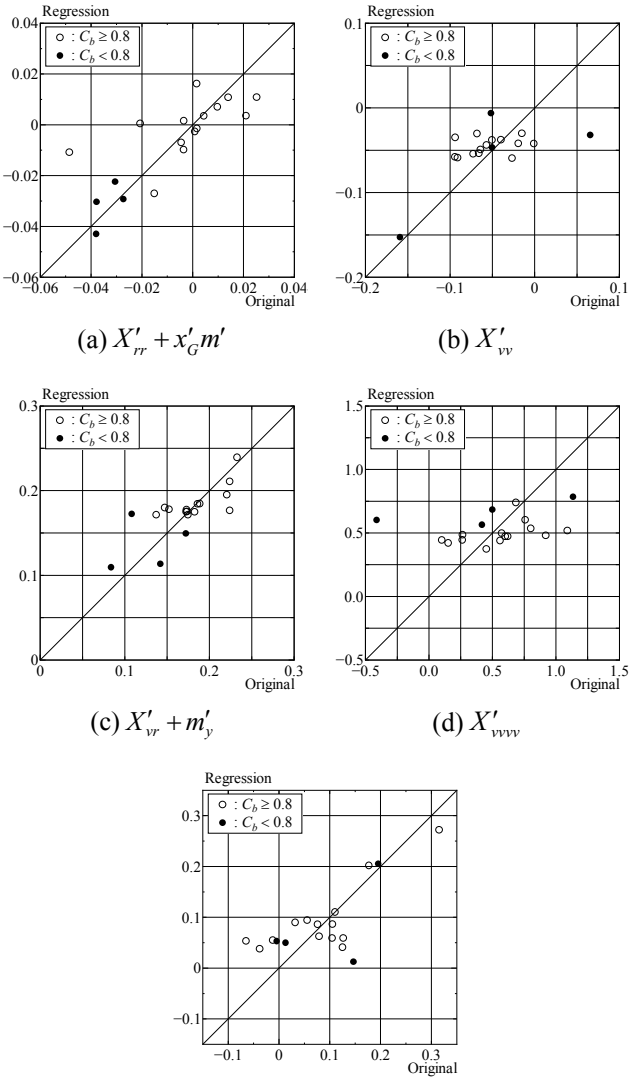

(a) $X'_{rr}+x'_Gm'$ (b) X'_{vv}

(c) $X'_{vr}+m'_y$ (d) X'_{vvvv}

(e) X'_{vvr}

Figure 4. Scattering diagrams of measured and regression values of hydrodynamic derivatives.

Table 3. Correlation coefficients of each hydrodynamic derivative and corresponding non-dimensional parameter.

Derivatives	Parameters	Correlation coefficients
$X'_{rr}+x'_Gm'$	$(1-C_b)L/T$	0.55097
X'_{vv}	$(1-C_b)L/T$	0.40707
$X'_{vr}+m'_y$	$(1-C_b)B/L$	0.65634
X'_{vvvv}	$(L/B)^2$	0.30044
X'_{vvr}	$(L/T)^2$	0.36709

and a regression formula which has minimum AIC (Akaike Information Criterion) for each derivative was selected as the following,

$$X'_{rr}+x'_Gm' = -14.7T/L - 5.20C_bB/L + 107.8BTC_b/L^2 + 0.701 \quad (10)$$

Table 4. Correlation coefficients of each hydrodynamic derivative and C_bB/L.

Derivatives	Parameters	Correlation coefficients
$X'_{rr}+x'_Gm'$	C_bB/L	0.51695
X'_{vv}	C_bB/L	0.33612
$X'_{vr}+m'_y$	C_bB/L	0.41833
X'_{vvvv}	C_bB/L	0.26454
X'_{vvr}	C_bB/L	0.14153

$$X'_{vv} = 7.14C_b + 38.4B/L - 46.6C_bB/L - 5.94 \quad (11)$$

$$X'_{vr}+m'_y = 3.99C_bB/L + 0.0113(L/B)^2 - 0.755 \quad (12)$$

$$X'_{vvvv} = 0.0182(L/B)^2 - 0.0826 \quad (13)$$

$$X'_{vvr} = 0.664C_b - 2.92L/B + 0.253(L/B)^2 + 7.93 \quad (14)$$

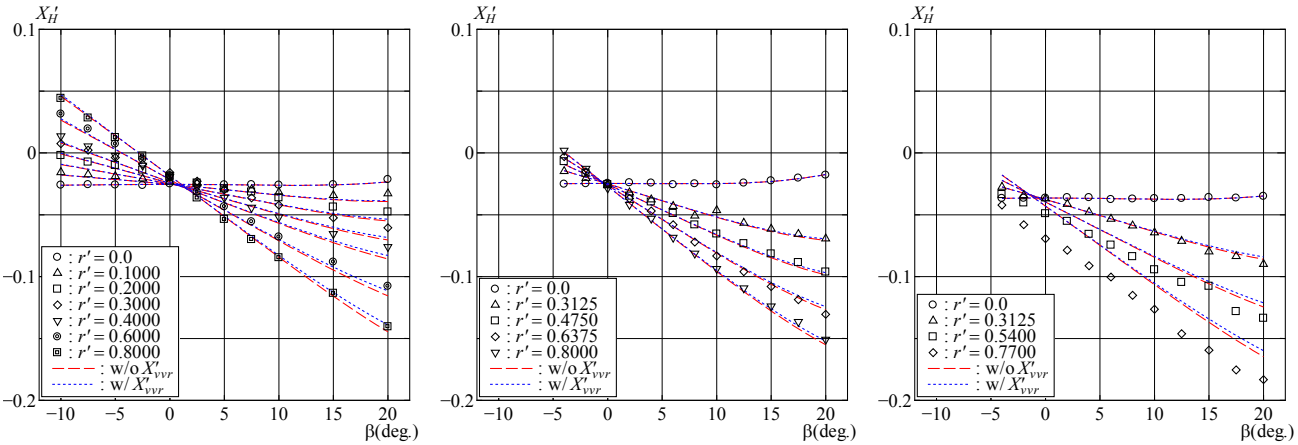

(a) Ship A (b) Ship C (c) Ship M

Figure 5. Regression curves calculated by using hydrodynamic derivatives estimated by Eqs.(10)-(14) in deep water condition (Ships A, C and M).

Figure 4 shows the scatter diagram of the measured and regression values of hydrodynamic derivatives. Although there are a few points which have low correlation between measured and regression values, most of regression values have good correlation with measured values. Fitting curves with the hydrodynamic derivatives for the ships A, C and M calculated by using Eqs.(10)-(14) are shown in Figure 5. Red broken lines and blue dotted lines represent estimated forces either without or with X'_{vvr} term respectively. Good agreement can be observed for the ships A and C, but large discrepancy exists at $\beta = 0°$ for the ship M. This arises from difference between measured and regression values of $X'_{rr} + x'_G m'$. The ship M has the largest value of $|X'_{rr} + x'_G m'|$, but Eq.(10) could not reproduce it.

4.3 HYDRODYNAMIC DERIVATIVES IN SHALLOW WATER CONDITIONS

The variation of hydrodynamic derivatives for the ratio of draught for water depth T/H is shown in Figure 6. The ratio of hydrodynamic derivatives in shallow water conditions for those in deep water condition is chosen as the vertical axis. Rough tendencies are observed in the variation of X'_{vv} and $X'_{vr} + m'_y$ for most of ships. They can be approximately formulated as the following,

$$\frac{[X'_{vv}]_{\text{shallow}}}{[X'_{vv}]_{\text{deep}}} = -70.8(T/H)^4 + 27.7(T/H)^2 + 1, \quad (15)$$

$$\frac{[X'_{vr} + m'_y]_{\text{shallow}}}{[X'_{vr} + m'_y]_{\text{deep}}} = 1.30(T/H)^2 + 1. \quad (16)$$

Fitting curves calculated by Eqs.(15) and (16) are shown in Figure 6 by black solid line.

On the other hand, it is difficult to find out the rough trends either in the variation of $X'_{rr} + x'_G m'$, X'_{vvvv} or X'_{vvr}. Although the ratio of $X'_{rr} + x'_G m'$ in shallow and deep water conditions takes a large value, the order of the derivative is relatively small comparing with other derivatives and the variation of the value in itself is not so

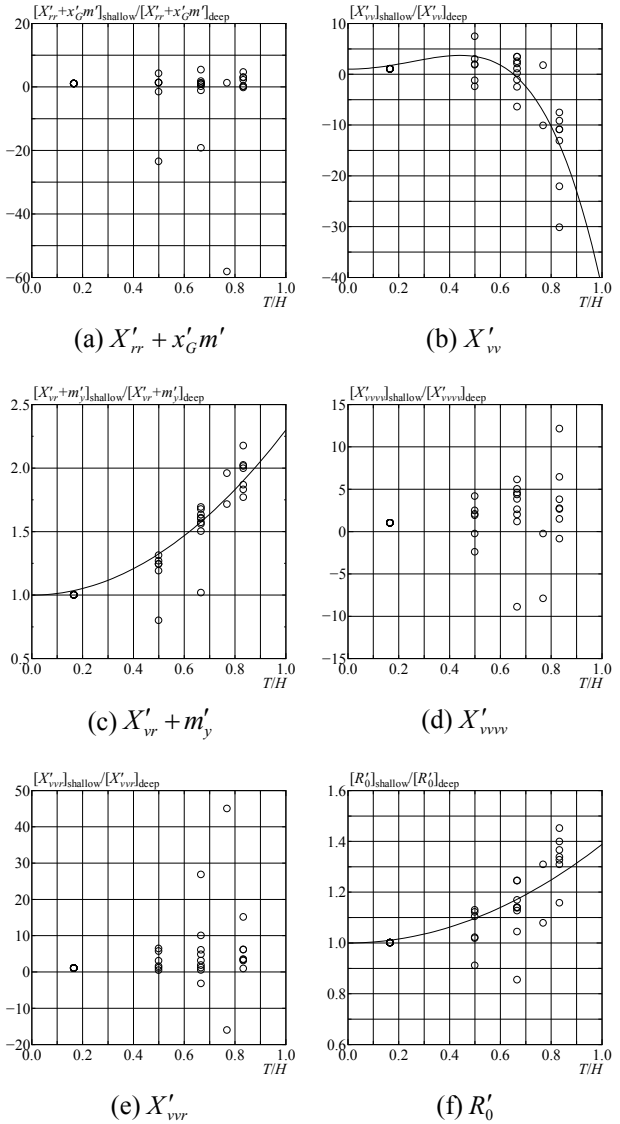

(a) $X'_{rr} + x'_G m'$ (b) X'_{vv}

(c) $X'_{vr} + m'_y$ (d) X'_{vvvv}

(e) X'_{vvr} (f) R'_0

Figure 6. Variation of hydrodynamic derivatives as function of *T*/*H*.

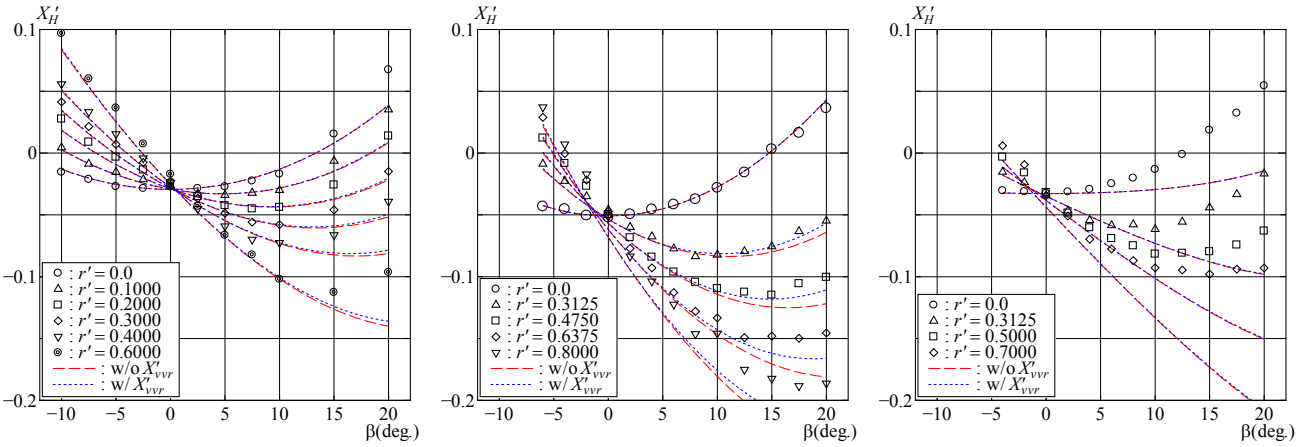

(a) Ship A (b) Ship E (c) Ship P

Figure 7. Regression curves calculated by using hydrodynamic derivatives estimated by Eqs.(10)-(16) in shallow water condition (Ships A, E and P, H/T = 1.2).

significant. Furthermore the contribution of X'_{vvvv} or X'_{vvr} to the total force is smaller than those of X'_{vv} and $X'_{vr} + m'_y$. So it may be possible to use the values of $X'_{rr} + x'_G m'$, X'_{vvvv} and X'_{vvr} in deep water condition instead of those in shallow water conditions.

Resistance coefficient R'_0 is also shown in Figure 6. It seems that the variation of R'_0 for T/H can be formulated roughly as the following,

$$\frac{[R'_0]_{\text{shallow}}}{[R'_0]_{\text{deep}}} = 0.388(T/H)^2 + 1. \qquad (17)$$

However, it would be desirable to use measured value of R'_0 in numerical simulation because R'_0 is the main component of longitudinal force and has much influence on simulation results.

Figure 7 shows fitting curves in shallow water condition (H/T = 1.2) with the hydrodynamic derivatives for the ships A, E and P calculated by using regression formulae shown by Eqs.(10)-(16). As stated above, shallow water effect on $X'_{rr} + x'_G m'$, X'_{vvvv} and X'_{vvr} are not considered in this figure and the measured value of R'_0 is used instead of using Eq.(17). Within the range where the values of drift angle and non-dimensional yaw rate are small, agreement between measured and estimated results is not so bad, but a difference gradually grows with the increase of drift angle and non-dimensional yaw rate and the degree of discrepancy varies according to ships. Significant discrepancy is observed for the ship P of which C_b is 0.7513.

5 CONCLUSIONS

Shallow water effects on the longitudinal components of hydrodynamic derivatives were investigated based on the analyses of hydrodynamic forces measured both in deep and shallow water conditions and regression formulae for the hydrodynamic derivatives as function of non-dimensional explanatory variables were presented. The regression formulae would be applicable for ships of which C_b is about 0.8 or more, because most of ships included in the database used for the analysis are bulk carriers and tankers having large C_b.

Furthermore, the variation of the longitudinal components of hydrodynamic derivatives for the water depth to draught ratio was shown. It was observed that the values of nonlinear derivatives change significantly depending on ships, hence further investigation on the influence of shallow water on the derivatives is necessary.

6 REFERENCES

1. Maimun, A.; Priyanto, A.; Rahimuddin; Baidowi, A.; Nurcholis (2009). Ship Manoeuvring in Shallow Water with Ship-bank Interaction Effects. *Proceedings of International Conference on Ship Manoeuvring in Shallow and Confined Water: Bank Effects*: pp.101–106.

2. Kim, S.W.; Kim, D.J.; Yeo D.J. (2009). Prediction of Manoeuvrability of a Ship at Low Forward Speed in Shallow Water. *Proceedings of International Conference on Ship Manoeuvring in Shallow and Confined Water: Bank Effects*: pp.147–152.

3. Yeo, D.J.; Yun, K.H.; Kim, Y.G.; Ryu, G.H. (2012). Manoeuvring Captive Model Tests of KCS Container Ship in Shallow Water. *Proceedings of 12th Asian Conference on Marine Simulator and Simulation Research (ACMSSR)*: 7pp.

4. Yoon, H.K.; Kang, S. (2013). Experimental Investigation on the Depth Effect of Hydrodynamic Coefficients Obtained by PMM Test in Square Tank. *Proceedings of 3rd International Conference on Ship Manoeuvring in Shallow and Confined Water: Ship Behaviour in Locks*: pp.209–214.

5. Yeo, D.J.; Yun, K.; Kim, Y.G.; Kim, S.Y. (2013). Benchmark HPMM Tests for KCS in Shallow Water. *Proceedings of 3rd International Conference on Ship*

Manoeuvring in Shallow and Confined Water: Ship Behaviour in Locks: pp.249–255.

6. Yeo, D.J. (2013). Investigation of the Depth Dependency of Manoeuvring Coefficients of KCS based on Captive Model Test Results. *Proceedings of 13th Asian Conference on Maritime System and Safety Research (ACMSSR)*: 6pp.

7. Simonsen, C.D.; Stern, F.; Agdrup, K. (2006). CFD with PMM Test Validation for Manoeuvring VLCC2 Tanker in Deep and Shallow Water. *Proceedings of International Conference on Marine Simulation and Ship Manoeuvrability (MARSIM) 2006*: 11pp.

8. Wang, H.M.; Zou, Z.J.; Yao, J.X. (2009). RANS Simulation of the Viscous Flow around a Turning Ship in Shallow Water. *Proceedings of International Conference on Marine Simulation and Ship Manoeuvrability (MARSIM) 2009*: 6pp.

9. Wang, H.M.; Zou, Z.J.; Tian, X.M. (2009). Numerical Simulation of the Viscous Flow around a Ship Undergoing Unsteady Berthing in Shallow Water, *Proceedings of International Conference on Ship Manoeuvring in Shallow and Confined Water: Bank Effects*: pp.121–126.

10. Kimura, Y.; Kobayashi, E.; Tahara, Y.; Koshimura, S. (2011). A Study on Estimation of Hydrodynamic Forces Acting on a Ship Hull in Shallow Water by CFD. *Proceedings of 2nd International Conference on Ship Manoeuvring in Shallow and Confined Water: Ship to Ship Interaction*: pp.193–201.

11. Furukawa, Y.; Nakiri, Y.; Kijima, K. (2011). *Proceedings of 2nd International Conference on Ship Manoeuvring in Shallow and Confined Water: Ship to Ship Interaction*: pp.147–152.

12. Hasegawa, K. (1980). On a Performance Criterion of Autopilot Navigation. *Journal of the Kansai Society of Naval Architects, Japan* No. 178: pp.93–103.

13. Yoshimura, Y.; Masumoto, Y. (2011). Hydrodynamic Force Database with Medium High Speed Merchant Ships Including Fishing Vessels and Investigation into a Manoeuvring Prediction Method (written in Japanese). *Journal of the Japan Society of Naval Architects and Ocean Engineers* Vol. 14: pp.63–73.

14. Yoshimura, Y. (1988). Mathematical Model for the Manoeuvring Ship Motion in Shallow Water (2nd Report) –Mathematical Model at Slow Forward Speed– (written in Japanese). *Journal of the Kansai Society of Naval Architects, Japan* No. 210: pp.77–84.

15. Eloot, K. (2006). Selection, Experimental Determination and Evaluation of a Mathematical Model for Ship Manoeuvring in Shallow Water. *PhD thesis, Ghent University*

16. Delefortrie, G. (2007). Manoeuvring Behaviour of Container Vessels in Muddy Navigation Areas. *PhD thesis, Ghent University*

17. Kijima, K.; Katsuno, T.; Nakiri, Y.; Furukawa, Y. (1990). On the Manoeuvring Performance of a Ship with the Parameter of Loading Condition. *Journal of the Society of Naval Architects of Japan* Vol. 168: pp.141–148.

18. Yasukawa, H.; Yoshimura, Y. (2015). Introduction of MMG Standard Method for Ship Maneuvering. *Journal of Marine Science and Technology* Vol. 20: pp.37–52.

19. Terada, D.; Yasukawa, H.; Furukawa, Y. (2013). A Regressive Model of Maneuvering Hydrodynamic Derivatives Using Hull Principal Particulars (written in Japanese). *Conference Proceedings of the Japan Society of Naval Architects and Ocean Engineers* Vol. 16: pp.13–15.

7 AUTHORS' BIOGRAPHIES

Yoshitaka Furukawa holds the current position of professor at Department of Marine Systems Engineering, Faculty of Engineering, Kyushu University. He is responsible for the research and education of ship dynamics.

Hiroshi Ibaragi holds the current position of assistant professor at Department of Marine Systems Engineering, Faculty of Engineering, Kyushu University. He is responsible for the research and education of ship dynamics.

Yasuaki Nakiri holds the current position of technical staff at Department of Marine Systems Engineering, Faculty of Engineering, Kyushu University. He is responsible for the execution of model experiment and data analysis at the Seakeeping and Manoeuvring Basin.

Katsuro Kijima is emeritus professor of Kyushu University. His previous experience includes the member of 19th and 20th ITTC Manoeuvring Committee and the chairman of 21st ITTC Manoeuvring Committee.